NASA CONTRACTOR REPORT

NASA CR-141424

BACKSCATTERING FROM A GAUSSIAN DISTRIBUTED, PERFECTLY CONDUCTING, ROUGH SURFACE

G. S. Brown

Prepared Under Contract No. NAS6-2520 by

Applied Science Associates, Inc.
105 East Chatham Street
Apex, North Carolina 27502

National Aeronautics and Space Administration

Wallops Flight Center
Wallops Island, Virginia 23337
AC 804 824-3411

August 1977

1. Report No.	2. Government Accession No.	3. Recipient's Catalog No.
NASA CR-141424		

4. Title and Subtitle	5. Report Date
BACKSCATTERING FROM A GAUSSIAN DISTRIBUTED, PERFECTLY CONDUCTING, ROUGH SURFACE	August 1977
	6. Performing Organization Code
7. Author(s)	8. Performing Organization Report No.
G. S. Brown	
	10. Work Unit No.
9. Performing Organization Name and Address	
Applied Science Associates, Inc. 105 East Chatham Street Apex, North Carolina 27502	11. Contract or Grant No. NAS6-2520
	13. Type of Report and Period Covered Contractor Report 1/20/76-1/20/77
12. Sponsoring Agency Name and Address	14. Sponsoring Agency Code
National Aeronautics and Space Administration Wallops Flight Center Wallops Island, Virginia 23337	

15. Supplementary Notes

16. Abstract

This report presents an analytical approach to the problem of scattering by random surfaces possessing many scales of roughness. The approach is applicable to bistatic scattering from dielectric surfaces, however, this specific analysis is restricted to backscattering from a perfectly conducting surface in order to more clearly illustrate the method. The surface is assumed to be Gaussian distributed so that the surface height can be split into large ζ_ℓ and small ζ_s scale components, relative to the electromagnetic wavelength. A first order perturbation approach is employed wherein the scattering solution for the large scale structure is perturbed by the small scale diffraction effects. The scattering from the large scale structure is treated via geometrical optics techniques since $4k_o^2 \overline{\zeta_\ell^2} \gg 1$. To the accuracy of the first order perturbation theory, the assumption of two-scale scattering, and k_o large, the resulting solution is essentially exact. The effect of the large scale surface structure is shown to be equivalent to a convolution in k-space of the height spectrum with the following: the shadowing function, a polarization and surface slope dependent function, and a Gaussian factor resulting from the unperturbed geometrical optics solution. This solution provides a continuous transition between the near normal incidence geometrical optics and wide angle Bragg scattering results. A specific example indicates that the large and small scale separation wavenumber should be based on the condition $4k_o \overline{\zeta_s^2} \approx 1$.

17. Key Words (Suggested by Author(s))	18. Distribution Statement
Rough surface scattering Scattering from ocean surface Electromagnetic scattering from stochastic surfaces	Unclassified - unlimited STAR Category 35

19. Security Classif. (of this report)	20. Security Classif. (of this page)	21. No. of Pages	22. Price*
Unclassified	Unclassified	44	

*For sale by the National Technical Information Service, Springfield, Virginia 22151

CONTENTS

1.0 INTRODUCTION AND SUMMARY OF RESULTS

Classical analyses of random rough surface scattering [1] are capable of providing precise quantitative predictions for two distinctly different types of surfaces; the gently undulating surface having large surface height excursions, and the surface characterized by small height and slope excursions. For the former case, the solution assumes the validity of the physical optics approximation for the current induced on the surface by the incident electromagnetic fields; it, therefore, comprises a high frequency solution to the scattering problem. In the case of the latter surface, a boundary perturbation technique is employed and the resulting solution represents a low frequency limiting form. That is, the height of the surface perturbations must be small relative to the electromagnetic wavelength. The physical optics approach can be applied to surfaces having small height excursions, however, such an application does not yield the proper polarization dependence.

For surfaces characterized by many scales* of roughness, the so-called composite surface scattering theory [2,3,4] has been developed as a means for predicting the behavior of the electromagnetic fields scattered by the surface. In this approach, the scattering in the near-specular direction is dominated by the physical optics solution, whereas the large angle of incidence perturbation contribution is modified due to local tilting of the mean flat surface by the large scale surface components. The total average scattered power is the incoherent sum of the physical optics and the

---

*The terminology large scale and small scale refers, approximately, to the height of the surface excursions. The large scale heights are measured relative to the mean flat surface. The small scale heights are measured relative to the large scale surface (see Figure 1). A more precise definition in terms of the surface height spectrum will be given in section 2.0.

tilted perturbation solutions with restrictions (in observation space) on the regions of validity of the sum. More recently, an alternate attack on the problem of scattering by a surface with many scales of roughness has been proposed [5]; however, the basic approach employed in the analysis has been seriously questioned [6]. Although the composite model of scattering by surfaces possessing many scales of roughness is very satisfying for small and large angles of incidence, i.e. where either the physical optics or the perturbation solutions are dominant, it would seem that additional analytical effort is required for the transition region between the two solutions.

The original intent of this investigation was to find a solution to the composite surface scattering problem which provided for a continuous transition between the near specular physical optics and wide angle tilted plane Bragg solutions. As will be shown, the results obtained herein not only describe the transition, but, to the accuracy of (1) the first order perturbation theory, (2) large electromagnetic wavenumber, and (3) the inclusion of only physical optics or small scale diffraction*, are essentially exact. Unlike the conventional composite surface scattering theory, the present approach is based on analytical techniques rather than physical considerations; the physical considerations are introduced after the final result is obtained in order to verify known limiting behavior.

The analysis employs a perturbation technique developed by Burrows [7, 8,9] which, because of its simplicity, is the key to the entire solution. The zeroth order solution is taken to be the physical optics scattering result while the first order perturbation term uses the physical optics result

*Surface features such as edges and cusps are not amenable to analysis by first order perturbation theory and are not considered here.

as the unperturbed solution. In order to use this particular approach, the surface height spectrum must be split into two contiguous regions; the large scale surface height (ζ_ℓ) represented by the low frequency region is assumed to be sufficiently smooth so as to form the unperturbed surface. This unperturbed surface is amenable to a physical optics approach for determining the scattered fields. The small scale surface height (ζ_s) represented by the high frequency part of the spectrum is assumed sufficiently small so that a first order perturbation of the physical optics solution is an adequate description of its scattering properties. Since the analysis also requires that ζ_ℓ and ζ_s be independent, the surface is assumed to be jointly Gaussian. The use of spectral dichotomy introduces a dependence in the solution upon the wavenumber where the spectral splitting occurs (k_d). This wavenumber cannot be completely specified, but it can be bounded from one side by the small height requirement on ζ_s, i.e. $4k_o^2 \overline{\zeta_s^2} << 1$, where k_o is the electromagnetic wavenumber and $\overline{\zeta_s^2}$ is the mean square height of the small scale structure. However, physical considerations are introduced to show that k_d can, in fact, be rather tightly specified. The specification of k_d will depend upon the surface height spectrum.

In order not to overly obscure the basic approach, the analysis is restricted to the case of backscattering from a perfectly conducting surface; the extension to bistatic scattering from a dielectric interface follows essentially the same procedures. The evaluation of the first order perturbation mean square power, including shadowing, is greatly facilitated by identities developed by Stogryn [10] and Sancer [15]. Using Fourier transform techniques, the first order perturbation scattering for $4k_o^2 \overline{\zeta_\ell^2} >> 1$ is shown to comprise two terms. The first involves a convolution in the wavenumber domain of the surface height spectrum, a polarization dependent

function, a shadowing function, and a Gaussian function whose width is determined by the large scale mean square slopes. The second term is identical to the first except that the convolution integration is over a finite domain which, in turn, is determined by the wavenumber k_d. The sum of these two terms along with the geometrical optics* result provide for a continuous description of the scattering. Under the assumption of small large scale mean square slopes, the result is essentially identical to the conventional composite surface result except in the transition region between the geometrical optics and first order perturbation terms. When the large scale slopes are not small, the two results are not in obvious agreement; however, a numerical comparison would be required to determine the degree of error in the conventional result.

For an isotropic height spectrum and small large scale slopes, the result reduces to a particularly simple form. A numerical example is presented wherein the behavior of the solution is studied as a function of the wavenumber k_d. Based on the criteria that k_d be as small as possible (to insure that the large scale surface is sufficiently smooth) and that $4k_o^2 \overline{\zeta_s^2} \ll 1$, the results of this example indicate that k_d should be chosen according to $4k_o^2 \overline{\zeta_s^2} \approx 0.1$. Using this criterion and $\lambda_o = 2$ cm, λ_d was computed to be 2π cm. That is, the geometrical optics solution is assumed to be accurate for all surface features having wavelengths greater than $3\lambda_o$ while the first order perturbation term is assumed to be valid for all features having wavelengths less than $3\lambda_o$. To the accuracy of the basic scattering mechanism assumption, i.e. geometrical optics or small scale diffraction, this computed value of λ_d appears to be reasonable.

---

*Since it was necessary to assume that $4k_o^2 \overline{\zeta_\ell^2} \gg 1$, the physical optics scattering is equivalent to the geometrical optics limit.

In addition to the continuous transition property of this result, it also exhibits two other important features. As the electromagnetic wavelength, λ_o, increases then so must λ_d. Consequently, the large scale mean square slopes will decrease and the geometrical optics result will increase at normal incidence and decay more rapidly with angle of incidence. Hence, there will be a frequency dependence in the geometrical optics result which is not predicted by conventional Kirchhoff analysis but has been experimentally observed in radar studies of the moon [11]. The use of a truncated spectrum in calculating the (geometrical optics) effective mean square slopes was originally proposed by Hagfors [12]; such an approach has now been verified and explained. It will also be shown that the first order perturbation result gives rise to depolarization which is dependent on the large scale slope; when the large scale slope is small, the depolarization is essentially zero, however, when these slopes are large the depolarization may not be negligible especially near grazing incidence. Further calculations are required to adequately assess the degree of depolarization.

2.0 SURFACE DESCRIPTION

The scattering surface is taken to be perfectly conducting and infinite in extent along the x and y coordinate axes (see Figure 1). The height of the surface $z = \zeta(x,y)$ is measured with respect to the $z = 0$ plane which is chosen such that the average height of the rough surface is zero, i.e. $\overline{\zeta(x,y)} = 0$. The random surface height $\zeta(x,y)$ is assumed to comprise a <u>superposition</u> of a sufficiently large number of zero mean, independent "component" heights so that $\zeta(x,y)$ and all of its derivatives are Gaussian [13]. In addition, the surface is assumed to be free of edges or cusps since such features are not adequately accounted for by the theory to be presented [7]. The spectrum of

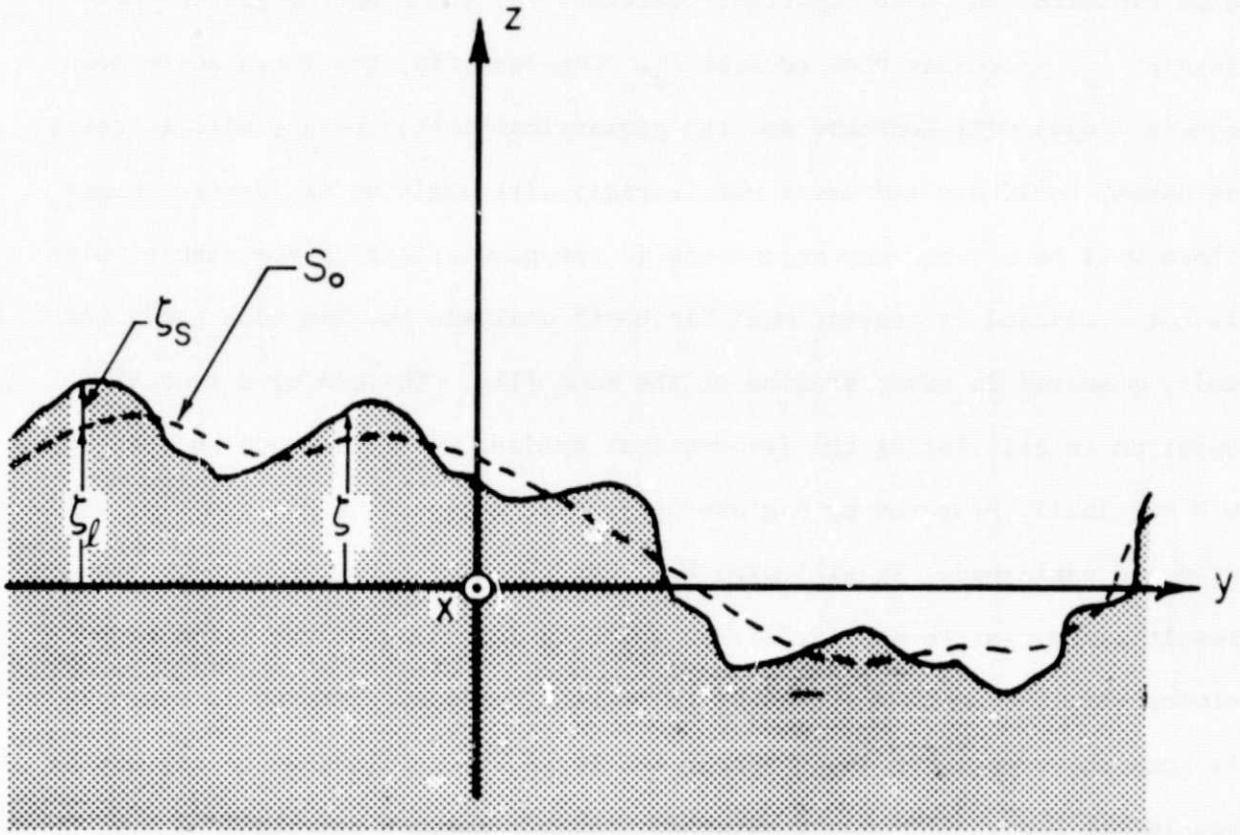

Figure 1. Composite surface ζ as a superposition of large (ζ_ℓ) and small scale (ζ_s) undulations. The z = 0 plane corresponds to the mean surface. The surface S_o is the unperturbed (large scale) surface.

the surface height undulations is given by $S(k_x,k_y)$ where k_x and k_y are wavenumbers along the x and y-directions, respectively. Since $\zeta(x,y)$ is a linear sum of statistically independent "component" heights, the sum may be rearranged into the following form:

$$\zeta(x,y) = \zeta_\ell(x,y) + \zeta_s(x,y) \tag{1}$$

where ζ_ℓ and ζ_s are also independent, zero mean, Gaussian processes. The spectrum for $\zeta_\ell(x,y)$ is $S(k_x,k_y)$ for $(|k_x| \leq k_d) \cap (|k_y| \leq k_d)$, while the spectrum for $\zeta_s(x,y)$ is $S(k_x,k_y)$ for $(|k_x| > k_d) \cup (|k_y| > k_d)$. The choice of the wavenumber k_d is such that the following two requirements are satisfied for the large and small scale surfaces, respectively;

$$4k_o^2 \, \overline{\zeta_\ell^2} \gg 1 \quad , \tag{2}$$

$$4k_o^2 \, \overline{\zeta_s^2} \ll 1 \; ; \; \left|\frac{\partial \zeta_s}{\partial x}\right| = |\zeta_{sx}| < 1 \; ; \; \left|\frac{\partial \zeta_s}{\partial y}\right| = |\zeta_{sy}| < 1 \tag{3}$$

where k_o is the wavenumber of the electromagnetic field incident upon the rough surface. In addition to (2), it is implicitly assumed that for the large scale surface, i.e., $\zeta_\ell(x,y)$, the radius of curvature is everywhere large relative to the electromagnetic wavelength $\lambda_o = 2\pi/k_o$. Since $\zeta_\ell(x,y)$ and $\zeta_s(x,y)$ are independent, the surface height spectrum may be expressed as follows:

$$S(k_x,k_y) = S_\ell(k_x,k_y) + S_s(k_x,k_y) \tag{4}$$

where

$$S_\ell(k_x,k_y) = S(k_x,k_y) \qquad (|k_x| \leq k_d) \cap (|k_y| \leq k_d) \tag{5}$$

$$S_s(k_x,k_y) = S(k_x,k_y) \qquad (|k_x| > k_d) \cup (|k_y| > k_d) \tag{6}$$

Equations (1) and (4) along with the fact that ζ_ℓ and ζ_s are zero mean Gaussian are crucial to the development to follow. If $\zeta(x,y)$ is non-Gaussian, it is not clear that the densities of ζ_ℓ and ζ_s and their derivatives can be uniquely defined [14]. More importantly, however, is the fact that spectral dichotomy as given by (4) may be invalid. That is, if $\zeta(x,y)$ is non-Gaussian then either it is not a linear superposition of the "component" surface heights or there is not a sufficient number of statistically independent "component" heights, and either of these conditions would invalidate (4). The analysis presented here requires Gaussian statistics. When the large scale slopes are small, the Gaussian assumption can be removed provided spectral dichotomy is still applicable; however, the analysis would necessarily have to be modified. For the case of the ocean surface, nonlinearities are a major source of concern and their effects are required to be small for this analysis to hold.

The purpose of the above discussion is to set the stage for the application of Burrows' perturbation technique to the computation of the fields scattered by the random surface. For k_d sufficiently small relative to k_o (the electromagnetic wavenumber), the artificial surface $z = \zeta_\ell(x,y)$ will be gently undulating and will, therefore, be amenable to a physical optics analysis for the scattered fields. Assuming that (3) can also be satisfied, the small scale surface height $\zeta_s(x,y)$ can be treated as a slight disturbance of $\zeta_\ell(x,y)$, and the first order perturbation of the physical optics fields can be computed using Burrows' most recent formulation [9]. The technique of perturbing the physical optics solution to account for small amplitude surface distortions has previously been applied to deterministic scattering by a large sphere, and

excellent agreement with numerical solutions were obtained [7]. It can also be shown that for a slightly perturbed planar surface, Burrows' theory results in the classical Rice solution with a considerable reduction in mathematical manipulations. In essence, Burrows has provided the formalism required to solve the composite surface scattering problem to the accuracy of first order perturbation theory; this paper presents the details necessary to go from formalism to results.

3.0 APPLICATION OF BURROWS' PERTURBATION THEORY

Burrows has shown that for a perfectly conducting scatterer, the first order perturbation scattered field, $\delta\vec{E}^1$, is given by the following expression [(3) of 9]:

$$\delta\vec{E}^1 \cdot \vec{j}' = j\omega_o 4 \int \left(\varepsilon_o \hat{n} \cdot \vec{E}_i \, \hat{n} \cdot \vec{E}_i' + \mu_o \hat{n} \times \vec{H}_i \cdot \hat{n} \times \vec{H}_i' \right) \zeta_s dS_o \qquad (7)$$

where the unprimed fields are incident fields evaluated at the unperturbed surface S_o, and the primed fields are incident fields evaluated at S_o due to an electric current element $\vec{j}'$ at a distance r from the surface. The unperturbed surface S_o is assumed to be sufficiently smooth for the application of the physical optics assumption. Also, $\hat{n}$ is the outward directed normal to the unperturbed surface, ω_o is the radian frequency of the incident field, and ε_o, μ_o are constitutive parameters of free space surrounding the scattering surface. The prime and unprime notation refer to different coordinate systems; a convenient shorthand notation for bistatic scattering and principal or cross polarization sampling. For the purposes of this paper, it is more convenient to replace $\vec{j}'$ by an equivalent plane wave [7]; then, using

$$\vec{H}_i = \left(\frac{\varepsilon_o}{\mu_o}\right)^{1/2} \hat{k}_i \times \vec{E}_i \quad ,$$

and letting the primed and unprimed coordinates be identical, i.e., backscattering, (7) simplifies to the following form;

$$\delta\vec{E}^1 \cdot \vec{E}'_o = \frac{k_o^2}{\pi r} \exp(-jk_o r) \int \left[2(\hat{n}\cdot\vec{E}_i)(\hat{n}\cdot\vec{E}'_i) + (\hat{n}\cdot\hat{k}_i)^2(\vec{E}_i\cdot\vec{E}'_i)\right] \zeta_s \, dS_o \qquad (8)$$

The primes in (8) now imply a possibly different polarization than the unprimed fields. The quantity $\vec{E}'_o$ is the reference amplitude and polarization of the (primed) field. For the principally polarized component of $\delta\vec{E}^1$, $\vec{E}\cdot\vec{E}' = E^2$, while for the cross polarized component of $\delta\vec{E}^1$, $\vec{E}\cdot\vec{E}' = 0$. The unprimed fields have the same reference amplitude as the primed fields, i.e., E_o. In (8), $\hat{k}_i$ specifies the propagation direction of the incident fields.

The orientation of the plane of incidence (and scattering) relative to the surface referenced coordinate system is shown in Figure 2. The incident wave vector is at an angle θ with respect to the z-axis, and its direction relative to the x-axis is specified by the angle ϕ. For the present, the orientation of the x and y-axis is arbitrary, however, it will be fixed by subsequent considerations. The wave vector is given by

$$\vec{k}_i = k_o \hat{k}_i = k_o(-\sin\theta\cos\phi\,\hat{x} - \sin\theta\sin\phi\,\hat{y} - \cos\theta\,\hat{z}) \qquad (9)$$

while a position vector from the origin to any point on S_o is given as

$$\vec{r}_s = x\,\hat{x} + y\,\hat{y} + \zeta_s\,\hat{z} \qquad (10)$$

The unit normal to the unperturbed surface S_o is

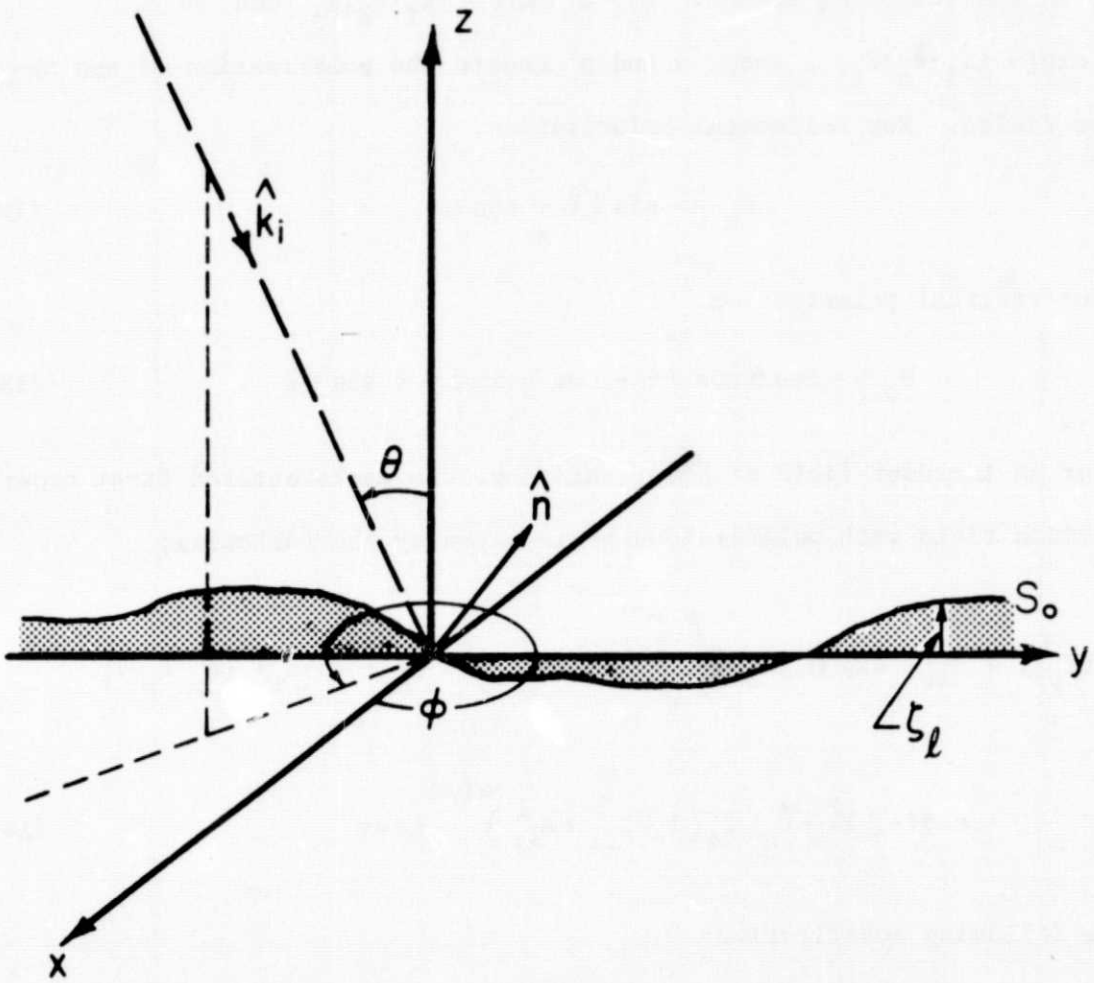

Figure 2. Orientation of the plane of incidence (and scattering) relative to the surface referenced coordinate system.

$$\hat{n} = \frac{-\zeta_{\ell x}\hat{x} - \zeta_{\ell y}\hat{y} + 1\hat{z}}{\sqrt{1+\zeta_{\ell x}^2+\zeta_{\ell y}^2}} \quad . \tag{11}$$

The prime and unprime incident electric fields at the surface S_o may be expressed in the following manner: $\vec{E}_i = E_o \exp(-j\vec{k}_i\cdot\vec{r}_o)\hat{e}_p$ and $\vec{E}_i' = E_o \exp(-j\vec{k}_i\cdot\vec{r}_o)\hat{e}_{p'}$, where p and p' denote the polarization of the respective fields. For horizontal polarization,

$$\hat{e}_h = -\sin\phi\,\hat{x} + \cos\phi\,\hat{y} \tag{12}$$

while for vertical polarization

$$\hat{e}_v = -\cos\theta\cos\phi\,\hat{x} - \cos\theta\sin\phi\,\hat{y} + \sin\theta\,\hat{z} \quad . \tag{13}$$

Thus, for an incident field of polarization p, the backscattered first order perturbation field with polarization p' is given by the following;

$$\delta E^1_{pp'} = \frac{E_o k_o^2}{\pi r}\exp(-jk_o r)\iint\left[2(\hat{n}\cdot\hat{e}_p)(\hat{n}\cdot\hat{e}_{p'}) + (\hat{n}\cdot\hat{k}_i)^2(\hat{e}_p\cdot\hat{e}_{p'})\right]$$

$$\cdot\ \exp(-j2\vec{k}_i\cdot\vec{r}_o)\,\zeta_s\left(1+\zeta_{\ell x}^2+\zeta_{\ell y}^2\right)^{-1/2} dx\,dy \tag{14}$$

With the following substitution;

$$\Gamma_{pp'}(\zeta_{\ell x},\zeta_{\ell y}) = \frac{2(\hat{n}\cdot\hat{e}_p)(\hat{n}\cdot\hat{e}_{p'}) + (\hat{n}\cdot\hat{k}_i)^2(\hat{e}_p\cdot\hat{e}_{p'})}{\sqrt{1+\zeta_{\ell x}^2+\zeta_{\ell y}^2}} \tag{15}$$

equation (14) reduces to

$$\delta E^1_{pp'} = \frac{E_o k_o^2}{\pi r}\exp(-jk_o r)\iint\Gamma_{pp'}(\zeta_{\ell x},\zeta_{\ell y})\exp(-j2\vec{k}_i\cdot\vec{r}_o)\,\zeta_s\,dxdy \tag{16}$$

The zeroth order or physical optics field is given by [12]

$$\delta E^{0}_{pp'} = -j \frac{E_o k_o \delta_{pp'}}{2\pi r \cos\theta} \exp(-j k_o r) \iint \exp(-j 2\vec{k}_i \cdot \vec{r}_o)\, dxdy \qquad (17)$$

where

$$\delta_{pp'} = \begin{cases} 1 & p'=p \\ 0 & p' \neq p \end{cases}$$

The backscattered electric field with polarization p' for an incident field with polarization p is, therefore,

$$E_{pp'} \approx \delta E^{0}_{pp'} + \delta E^{1}_{pp'} \quad . \qquad (18)$$

The accuracy of (18) is dependent upon the accuracy of the first order perturbation and, if (16) and (17) are used, the smoothness of the unperturbed surface S_o. From a more fundamental point of view, the accuracy is determined by the basic assumption of two scattering mechanisms, i.e. physical optics and small feature diffraction. Since edge diffraction need not be considered because the composite surface has been specified as free of edges, the two-scattering-mechanism formulation should be adequate.

The backscattering cross section per unit area is given by

$$\sigma^{\circ}_{pp'}(\theta,\phi) = \lim_{r\to\infty} \lim_{A_{ill}\to\infty} \left\{ \frac{4\pi r^2}{A_{ill}} \frac{\overline{|E_{pp'}|^2}}{E_o^2} \right\} \qquad (19)$$

where the over-bar denotes an ensemble average. Since ζ_s is a zero mean process, the cross products in (19) are zero and

$$\overline{|E_{pp'}|^2} = \overline{|\delta E^{0}_{pp'}|^2} + \overline{|\delta E^{1}_{pp'}|^2} \quad , \qquad (20)$$

and because ζ_s and ζ_ℓ are independent processes,

$$\sigma^{\circ}_{pp'}(\theta,\phi) = 2k_o^2\,\delta_{pp'}\sec^2\theta\,R(\theta,\phi)\int_{-\infty}^{\infty}\int_{-\infty}^{\infty}\exp(-j\,k_{ox}\Delta x - j\,k_{oy}\Delta y)$$

$$\cdot\,\exp\left\{-4k_o^2\cos^2\theta\,\overline{\zeta_\ell^2}\left[1-\rho_\ell(\Delta x,\Delta y)\right]\right\}d\Delta x\,d\Delta y$$

$$+\frac{4k_o^4}{\pi}\iint_{A_{ill}}\left\langle\Gamma_{pp'}\left(\zeta_{\ell x_1},\zeta_{\ell y_1}\right)\Gamma^{*}_{pp'}\left(\zeta_{\ell x_2},\zeta_{\ell y_2}\right)\exp\left[jB\left(\zeta_{\ell_1}-\zeta_{\ell_2}\right)\right]\right\rangle$$

$$\cdot\,\overline{\zeta_s^2}\,\rho_s(\Delta x,\Delta y)\exp(-j\,k_{ox}\Delta x - j\,k_{oy}\Delta y)\,d\Delta x\,d\Delta y \qquad (21)$$

The new functions in (21) are defined as follows; $R(\theta,\phi)$ is the shadowing function for the large scale surface [15], $\rho_\ell(\Delta x,\Delta y)$ is the normalized autocorrelation function for the large scale surface excursions, $k_{ox} = -2k_o\sin\theta\cos\phi$, $k_{oy} = -2k_o\sin\theta\sin\phi$, $B = 2k_o\cos\theta$, and $\rho_s(\Delta x,\Delta y)$ is the normalized autocorrelation function for the small scale structure. Multiplication of the physical optics term by $R(\theta,\phi)$ is justified by Sancer's [15] and Barrick's [16] analyses. That is, Sancer showed that the effect of shadowing on the slope density scattering result was equivalent to a multiplication by the function $R(\theta,\phi)$; Barrick had previously demonstrated that the slope density and physical optics results were equivalent for $4k_o^2\cos^2\theta\,\overline{\zeta_\ell^2} \gg 1$, i.e. the geometrical optics limit. Thus, the first term in (21) is strictly only valid in the geometrical optics limit and this restriction will be satisfied later in the analysis.

The integration in (21) is restricted to the projection of the illuminated areas of S_o onto the x-y plane [7]. Thus, the second term in (21) may be rewritten in the following form;

$$\left[\sigma^{\circ}_{pp'}(\theta,\phi)\right]_1 = \frac{4k_o^4}{\pi}\int_{-\infty}^{\infty}\int_{-\infty}^{\infty} \Big\langle I(x_1,y_1)I(x_2,y_2)f_{pp'}\left(\zeta_{\ell x_1},\zeta_{\ell x_2},\zeta_{\ell y_1},\zeta_{\ell y_2}\right)$$

$$\cdot \exp\left[jB\left(\zeta_{\ell_1}-\zeta_{\ell_2}\right)\right]\Big\rangle \overline{\zeta_s^2}\,\rho_s(\Delta x,\Delta y)$$

$$\cdot \exp\left(-j k_{ox}\Delta x - j k_{oy}\Delta y\right) d\Delta x\, d\Delta y \qquad (22)$$

where $I(x,y)$ is one if the point (x,y) on S_o is illuminated and zero if it is in shadow and the contributions from the shadow boundaries have been neglected. The function $f_{pp'}$ is merely equal to $\Gamma_{pp'}\left(\zeta_{\ell x_1},\zeta_{\ell y_1}\right)\Gamma^*_{pp'}\left(\zeta_{\ell x_2},\zeta_{\ell y_2}\right)$ and the notation $\left[\sigma^{\circ}_{pp'}(\theta,\phi)\right]_1$ implies the contribution of the first order perturbation to $\sigma^{\circ}_{pp'}(\theta,\phi)$. Equation (22) is the two dimensional Fourier transform of the product of the $\langle\cdot\rangle$ term and $\overline{\zeta_s^2}\,\rho_s(\Delta x,\Delta y)$. Hence, (22) is equal to the two dimensional convolution of the transforms. The transform of $\overline{\zeta_s^2}\,\rho_s(\Delta x,\Delta y)$ is just the spectrum $S(k_x,k_y)$ for $\left(|k_x|>k_d\right)\cup\left(|k_y|>k_d\right)$. The transform of a function having the same form as $\langle\cdot\rangle$ was first derived by Stogryn [10] under the assumption of no shadowing. Sancer [15] subsequently included shadowing, i.e. the I functions, and showed that, in the limit of $k_o\to\infty$, Stogryn's earlier result should be multiplied by the shadowing function $R(\theta,\phi)$. In particular, it is easily shown, using Stogryn's shadow corrected result, that

$$\frac{1}{2\pi}\int_{-\infty}^{\infty}\int_{-\infty}^{\infty}\left\langle I(x_1,y_1)I(x_2,y_2)f_{pp'}\left(\zeta_{\ell x_1},\zeta_{\ell x_2},\zeta_{\ell y_1},\zeta_{\ell y_2}\right)\exp\left[jB\left(\zeta_{\ell_1}-\zeta_{\ell_2}\right)\right]\right\rangle$$

$$\cdot \exp(-j k_{ox}\Delta x - j k_{oy}\Delta y)d\Delta x d\Delta y \approx R(\theta,\phi)f_{pp'}\left(\frac{k_{ox}}{B},\frac{k_{ox}}{B},\frac{k_{oy}}{B},\frac{k_{oy}}{B}\right)$$

$$\cdot \frac{1}{2\pi}\int_{-\infty}^{\infty}\int_{-\infty}^{\infty}\exp\left\{-j(k_{ox}\Delta x + k_{oy}\Delta y) - 4k_o^2\cos^2\theta\ \overline{\zeta_\ell^2}\ \left[1-\rho_\ell(\Delta x,\Delta y)\right]\right\} d\Delta x d\Delta y. \tag{23}$$

For no shadowing, i.e. $R(\theta,\phi)=1$, Stogryn demonstrated that (23) is valid provided <u>either</u> $4k_o^2\cos^2\theta\ \overline{\zeta_\ell^2} \gg 1$ <u>or</u> the large scale slopes are small.* However, in order to properly include the shadowing function, it will be necessary to be more restrictive. That is, (23) is strictly only true in the geometrical optics limit for only then is shadowing properly accounted for by the multiplicative factor $R(\theta,\phi)$. Hence, for all further analysis it will be necessary to require that $4k_o^2\cos^2\theta\ \overline{\zeta_\ell^2} \gg 1$. In addition, it is convenient at this point to fix the orientation of the x and y coordinate axes by requiring that $\overline{\zeta_{\ell xy}}=0$. Such a choice simplifies the details of the development to follow and also implies that the surface height spectrum has fold-over or mirror symmetry about <u>both</u> the $k_x=0$ and $k_y=0$ axes. Another consequence of this choice is that the direction of incidence, i.e. the angle ϕ, is now specified relative to the surface height spectrum.

The shadowing function for a anisotropic Gaussian surface was shown by Sancer [15] to have the following form; $R(\theta,\phi) = (1+C_o)^{-1}$ where

---

*The validity of (23) when the large scale slopes are small has recently been experimentally verified using backscattering measurements acquired by the Skylab radar altimeter [17].

$$2C_o = \left(\frac{2}{\pi}|\psi_o''|\right)^{1/2} \tan\theta \exp\left[-\frac{\mathrm{ctn}^2\theta}{2|\psi_o''|}\right] - \mathrm{erfc}\left[\frac{\mathrm{ctn}\,\theta}{(2|\psi_o''|)^{1/2}}\right] \tag{24}$$

and

$$\psi_o'' = -\overline{\zeta_{\ell x}^2}\cos^2\phi - \overline{\zeta_{\ell y}^2}\sin^2\phi \tag{25}$$

All terms in (23) involving ψ_o'' appear as $|\psi_o''|\tan^2\theta$ which can be rewritten as follows;

$$2|\psi_o''|\tan^2\theta = \frac{\overline{\zeta_{\ell x}^2}\, k_{ox}^2}{2k_o^2\cos^2\theta} + \frac{\overline{\zeta_{\ell y}^2}\, k_{oy}^2}{2k_o^2\cos^2\theta} \tag{26}$$

where, for clarity, the definitions of k_{ox} and k_{oy} are repeated below

$$\begin{aligned} k_{ox} &= -2k_o \sin\theta\cos\phi \\ k_{oy} &= -2k_o \sin\theta\sin\phi \end{aligned} \tag{27}$$

Using (26) and (24), the appropriate expression for $R(k_{ox},k_{oy})$ is given below

$$R\left(\frac{k_{ox}}{2k_o\cos\theta}, \frac{k_{oy}}{2k_o\cos\theta}\right) = \left\{\frac{1}{2\sqrt{\pi}}\left[2\left\{\overline{\zeta_{\ell x}^2}\left(\frac{k_{ox}}{2k_o\cos\theta}\right)^2 + \overline{\zeta_{\ell y}^2}\left(\frac{k_{oy}}{2k_o\cos\theta}\right)^2\right\}\right]^{1/2}\right.$$
$$\cdot \exp\left[-\frac{1}{2}\left\{\frac{1}{\overline{\zeta_{\ell x}^2}\left(\frac{k_{ox}}{2k_o\cos\theta}\right)^2 + \overline{\zeta_{\ell y}^2}\left(\frac{k_{oy}}{2k_o\cos\theta}\right)^2}\right\}\right]$$
$$\left. - \frac{1}{2}\,\mathrm{erfc}\left[\left\{\frac{1}{2}\left[\frac{1}{\overline{\zeta_{\ell x}^2}\left(\frac{k_{ox}}{2k_o\cos\theta}\right)^2 + \overline{\zeta_{\ell y}^2}\left(\frac{k_{oy}}{2k_o\cos\theta}\right)^2}\right]\right\}^{1/2}\right] + 1\right\}^{-1} \tag{28}$$

It should be noted, in (28), that there is no explicit restriction on the

angle of incidence to the range of $0° \leq \theta \leq 90°$. However, such a restriction is implied because $\theta > 90°$ would imply illumination of the surface from below the $z = 0$ plane. Therefore, for $-2k_o > k_{ox} > 2k_o$ and $-2k_o > k_{oy} > 2k_o$, the shadowing function in (28) is identically zero.

Thus, in order to completely specify the transform of the $\langle \cdot \rangle$ term in (22), it only remains to determine the transform of

$$\exp\left\{-4k_o^2 \cos^2\theta \; \overline{\zeta_\ell^2}\left[1 - \rho_\ell(\Delta x, \Delta y)\right]\right\} \quad .$$

Since $4k_o^2 \; \overline{\zeta_\ell^2} \cos^2\theta >> 1$, the large scale normalized autocorrelation function can be effectively approximated by a two term power series, i.e.

$$\rho_\ell(\Delta x, \Delta y) \approx 1 - \frac{1}{2}\left[\overline{\zeta_{\ell x}^2}\,(\Delta x)^2 + \overline{\zeta_{\ell y}^2}\,(\Delta y)^2\right] \tag{29}$$

Thus

$$\frac{1}{2\pi}\int_{-\infty}^{\infty}\int_{-\infty}^{\infty} \exp\left\{-j(k_{ox}\Delta x + k_{oy}\Delta y) - 4k_o^2 \cos^2\theta \; \overline{\zeta_\ell^2}\left[1 - \rho_\ell(\Delta x, \Delta y)\right]\right\} d\Delta x \, d\Delta y$$

$$\approx \frac{\left[\overline{\zeta_{\ell x}^2}\;\overline{\zeta_{\ell y}^2}\right]^{-1/2}}{4k_o^2 \cos^2\theta} \exp\left[-\frac{k_{ox}^2}{8k_o^2 \cos^2\theta \; \overline{\zeta_{\ell x}^2}} - \frac{k_{oy}^2}{8k_o^2 \cos^2\theta \; \overline{\zeta_{\ell y}^2}}\right] \tag{30}$$

where the specular term at normal incidence (which is implicit in the left hand side of (30)) has been ignored since $4k_o^2 \; \overline{\zeta_\ell^2} >> 1$ (see [10]). Combining (30), (28), and (24) the Fourier transform of the $\langle \cdot \rangle$ term in (22) is as follows:

$$\frac{1}{2\pi}\int_{-\infty}^{\infty}\int_{-\infty}^{\infty}\langle\cdot\rangle\exp(-jk_x\Delta x - jk_y\Delta y)\,d\Delta x\,d\Delta y = \frac{\left(\overline{\zeta_{\ell x}^2}\ \overline{\zeta_{\ell y}^2}\right)^{-1/2}}{4k_o^2\cos^2\theta}\cdot R\left(\frac{k_x}{2k_o\cos\theta}\ ,\ \frac{k_y}{2k_o\cos\theta}\right)$$

$$\cdot\ \Gamma_{pp}^2,\left(\frac{k_x}{2k_o\cos\theta}\ ,\ \frac{k_y}{2k_o\cos\theta}\right)\exp\left[\frac{-k_x^2}{8k_o^2\cos^2\theta\ \overline{\zeta_{\ell x}^2}} - \frac{k_y^2}{8k_o^2\cos^2\theta\ \overline{\zeta_{\ell y}^2}}\right] \tag{31}$$

for $4k_o^2\cos^2\theta\ \overline{\zeta_\ell^2} >> 1$. Using (31) and the fact that the transform of $\overline{\zeta_s^2}\ \rho_s(\Delta x,\Delta y)$ is $S(k_x,k_y)$ for $(|k_x| > k_d)\cup(|k_y| > k_d)$, the convolutional equivalent of (22) is

$$\left[\sigma^\circ_{pp},(\theta,\phi)\right]_1 = \frac{k_o^2\sec^2\theta}{\pi\left[\overline{\zeta_{\ell x}^2}\ \overline{\zeta_{\ell y}^2}\right]^{1/2}}\int_{-\infty}^{\infty}\int_{-\infty}^{\infty} S(k_x,k_y)\,R\left(\frac{k_{ox}-k_x}{2k_o\cos\theta}\ ,\ \frac{k_{oy}-k_y}{2k_o\cos\theta}\right)$$

$$\cdot\ \Gamma_{pp}^2,\left(\frac{k_{ox}-k_x}{2k_o\cos\theta}\ ,\ \frac{k_{oy}-k_y}{2k_o\cos\theta}\right)\exp\left[\frac{-(k_{ox}-k_x)^2}{8k_o^2\cos^2\theta\ \overline{\zeta_{\ell x}^2}} - \frac{(k_{oy}-k_y)^2}{8k_o^2\cos^2\theta\ \overline{\zeta_{\ell y}^2}}\right]dk_x\,dk_y$$

$$-\frac{k_o^2\sec^2\theta}{\pi\left[\overline{\zeta_{\ell x}^2}\ \overline{\zeta_{\ell y}^2}\right]^{1/2}}\int_{-k_d}^{k_d}\int_{-k_d}^{k_d} S(k_x,k_y)\ R\left(\frac{k_{ox}-k_x}{2k_o\cos\theta}\ ,\ \frac{k_{oy}-k_y}{2k_o\cos\theta}\right)$$

$$\cdot\ \Gamma_{pp}^2,\left(\frac{k_{ox}-k_x}{2k_o\cos\theta}\ ,\ \frac{k_{oy}-k_y}{2k_o\cos\theta}\right)\exp\left[\frac{-(k_{ox}-k_x)^2}{8k_o^2\cos^2\theta\ \overline{\zeta_{\ell x}^2}} - \frac{(k_{oy}-k_y)^2}{8k_o^2\cos\theta\ \overline{\zeta_{\ell y}^2}}\right]dk_x\,dk_y \tag{32}$$

The first term in (21) was evaluated in (30), i.e.

$$\left[\sigma^\circ_{pp},(\theta,\phi)\right]_0 = \frac{\delta_{pp},\sec^4\theta\ R(\theta,\phi)}{2\left[\overline{\zeta_{\ell x}^2}\ \overline{\zeta_{\ell y}^2}\right]^{1/2}}\exp\left[-\left(\frac{\cos^2\phi}{2\ \overline{\zeta_{\ell x}^2}} + \frac{\sin^2\phi}{2\ \overline{\zeta_{\ell y}^2}}\right)\tan^2\theta\right] \tag{33}$$

Since

$$\sigma^{\circ}_{pp'}(\theta,\phi) = \left[\sigma^{\circ}_{pp'}(\theta,\phi)\right]_0 + \left[\sigma^{\circ}_{pp'}(\theta,\phi)\right]_1 \tag{34}$$

the backscattering cross section per unit area is completely specified by the sum of (32) and (33). The derivation leading to (34) required only one assumption or condition, namely, $4k_o^2 \cos^2\theta\, \overline{\zeta_\ell^2} >> 1$. In the subsequent parts of this paper, interpretations of (34) will be presented which show that this condition can be violated when the slopes of the large scale surface structure are small. This fact confirms Stogryn's original observations even when shadowing is included.

4.0 COMPARISON WITH CONVENTIONAL COMPOSITE SURFACE THEORY

Equations (34), (33) and (32) represent the general expressions for the scattering from a Gaussian, perfectly conducting surface characterized by an anisotropic spectrum and possessing many scales of roughness. The accuracy of the result is dependent upon the large scale structure having large height excursions and small curvature, while the small scale structure must be characterized by small height and slopes.

The geometrical optics term given by (33) dominates the scattering near normal incidence. Except for the case when the large scale slopes are very large, the shadowing function has little effect on the result. The only important difference between (33) and previous results [15] is that (33) is determined by the large scale slope only; that is, the slope of the spectrum in the wavenumber range $(|k_x| \leq k_d) \cap (|k_y| \leq k_d)$. The wavenumber k_d is determined by the condition (on the small scale structure) that $4k_o^2 \overline{\zeta_s^2} << 1$; thus, as k_o changes, so also must k_d change in order to satisfy $4k_o^2 \overline{\zeta_s^2} << 1$. However, as k_d varies, $\overline{\zeta_{\ell x}^2}$ and $\overline{\zeta_{\ell y}^2}$ will also change. The net effect

of this process is to introduce a frequency dependence in (33) through the use of a truncated spectrum in computing the large scale slopes. The concept of a truncated or filtered spectrum was first hypothesized by Hagfors [12] in an attempt to explain lunar scattering data and the observed frequency dependence of near normal incidence scattering. More recently, Tyler [18] has attempted to definitize Hagfors filter theory by basing the spectral truncation wavenumber on a criterion related to the radius of curvature of the large scale surface. Both of these approaches base the point of spectral truncation upon a characteristic of the large scale structure, whereas, it should be based upon the small scale structure, i.e., $4k_o^2 \overline{\zeta_s^2} \ll 1$. The inadequacies in these earlier works probably stem from a failure to consider both types of appropriate scattering mechanisms, i.e. geometrical optics and small scale diffraction, and their proper combination.

In theory, the conventional composite surface scattering theory postulates a truncated spectrum for computing the large scale characteristics; however, little attention has been given to the fact that, as shown above, this will introduce a frequency dependence in the near normal incidence scattering. As is obvious from the above, the degree of frequency dependence is determined by k_o and the behavior of the spectrum in the small scale regime. Contrary to Hagfors original hypothesis, the wavenumber k_d does not depend upon the angle of incidence. Many of these points will be more clearly illustrated in the section of this paper dealing with a numerical example.

The perturbation term, given by (32), represents the effect of the small scale surface structure upon the scattering process. The convolutional form of (32) also clearly shows the primary impact of the large scale surface structure upon the small scale diffraction. That is, rather than depending upon a single Bragg wavenumber, (k_{ox}, k_{oy}), as in the case of no large scale

structure, (32) predicts that the scattering will result from a neighborhood of the Bragg wavenumber. The extent of this neighborhood is directly proportional to the mean square slopes of the large scale surface structure. The finite range integration in (32) insures that no Bragg scattering will result from spectral wavenumbers less than k_d. Since there is no small scale structure for $k \leq k_d$ by definition, the finite range integration must be included.

When $8k_o^2 \cos^2\theta \, \overline{\zeta_{\ell x}^2}$ and $8k_o^2 \cos^2\theta \, \overline{\zeta_{\ell y}^2}$ are small, the exponential factor in (32) is very peaked and it is dominant in the integrand. In this case, the integrals may be evaluated asymptotically using a form of Laplace's method [19] with the following result;

$$\left[\sigma^\circ_{pp'}(\theta,\phi)\right]_1 = \begin{cases} 0 & (|k_{ox}| \leq k_d) \cap (|k_{oy}| \leq k_d) \\ 8k_o^4 \, S(k_{ox},k_{oy}) R(0,0) \Gamma^2_{pp'}(0,0) & (|k_{ox}| > k_d) \cup (|k_{oy}| > k_d) \end{cases} \tag{35}$$

Since $R(0,0) = 1$, and

$$\Gamma^2_{pp'}(0,0) = \begin{cases} 0 & p = h,\ p' = v \text{ or } p = v,\ p' = h \\ \cos^4\theta & p = h,\ p' = h \\ (1+\sin^2\theta)^2 & p = v,\ p' = v \end{cases} \tag{36}$$

and $S(k_{ox},k_{oy}) = (\pi/2)W(k_{ox},k_{oy})^*$, where W is the spectral notation originally employed by Rice, (35) can be written as follows;

$$\left[\sigma^\circ_{pp'}(\theta,\phi)\right]_1 = \begin{cases} 0 & (|k_{ox}| \leq k_d) \cap (|k_{oy}| \leq k_d) \\ 4\pi k_o^4 \Gamma^2_{pp'}(0,0) W(k_{ox},k_{oy}) & (|k_{ox}| > k_d) \cup (|k_{oy}| > k_d) \end{cases} \tag{37}$$

*This results from the choice of symmetrical two dimensional Fourier transforms, in $1/(2\pi)$, for relating $S(k_x,k_y)$ and $\overline{\zeta^2}\,\rho(\Delta x,\Delta y)$.

In the absence of large scale structure, i.e., $\overline{\zeta_\ell^2} \to 0$, the entire surface comprises small scale height excursions and k_d may be set to zero; thus,

$$\lim_{\overline{\zeta_\ell^2} \to 0} \left[\sigma^\circ_{pp'}(\theta,\phi)\right]_1 = 4\pi k_o^4 \, \Gamma^2_{pp'}(0,0) \; W(-2k_o \sin\theta\cos\phi \, , -2k_o \sin\theta \sin\phi) \qquad (38)$$

with no restriction on the range of the argument of W. Equation (38) is the classical Rice solution for the backscattering from a slightly perturbed planar surface. This result demonstrates that in the absence of large scale surface height structure, (32) correctly predicts the scattering behavior. One further point of interest is the fact that the geometrical optics term in this limit contributes only a specular term at normal incidence, i.e.

$$\lim_{\overline{\zeta_\ell^2} \to 0} \left[\sigma^\circ_{pp'}(\theta,\phi)\right]_0 = \pi\delta_{pp'} \; \delta(\sin\theta\cos\phi)\,\delta(\sin\theta\sin\phi) \qquad (39)$$

where the term $\exp\left(-4k_o^2 \, \overline{\zeta^2}\right)$ does not appear because it is essentially unity, i.e. $4k_o^2 \, \overline{\zeta^2} = 4k_o^2\left(\overline{\zeta_\ell^2} + \overline{\zeta_s^2}\right) \ll 1$.

Under the following transformation of variables;

$$\xi_x = \frac{k_x - k_{ox}}{2k_o \cos\theta} \qquad\qquad \xi_y = \frac{k_y - k_{oy}}{2k_o \cos\theta} \quad ,$$

equation (32) assumes the form

$$\left[\sigma_{pp'}(\theta,\phi)\right]_1 = \frac{4k_o^4}{\pi\left[\overline{\zeta_{\ell x}^2}\;\overline{\zeta_{\ell y}^2}\right]^{1/2}} \int_{-\infty}^{\infty}\int_{-\infty}^{\infty} S(2k_o\cos\theta\,\xi_x + k_{ox}, 2k_o\cos\theta\,\xi_y + k_{oy})$$

$$\cdot\, R(-\xi_x,-\xi_y)\,\Gamma_{pp'}^2(-\xi_x,-\xi_y)\exp\left[-\frac{\xi_x^2}{2\overline{\zeta_{\ell x}^2}} - \frac{\xi_y^2}{2\overline{\zeta_{\ell y}^2}}\right] d\xi_x\, d\xi_y$$

$$- \frac{4k_o^4}{\pi\left[\overline{\zeta_{\ell x}^2}\cdot\overline{\zeta_{\ell y}^2}\right]^{1/2}} \int_{a_y}^{b_y}\int_{a_x}^{b_x} S(2k_o\cos\theta\,\xi_x + k_{ox}, 2k_o\cos\theta\,\xi_y + k_{oy})$$

$$\cdot\, R(-\xi_x,-\xi_y)\,\Gamma_{pp'}^2(-\xi_x,-\xi_y)\exp\left[-\frac{\xi_x^2}{2\overline{\zeta_{\ell x}^2}} - \frac{\xi_y^2}{2\overline{\zeta_{\ell y}^2}}\right] d\xi_x\, d\xi_y \qquad (40)$$

where

$$a_x = \frac{-k_d - k_{ox}}{2k_o\cos\theta} \qquad b_x = \frac{k_d - k_{ox}}{2k_o\cos\theta}$$

$$a_y = \frac{-k_d - k_{oy}}{2k_o\cos\theta} \qquad b_y = \frac{k_d - k_{oy}}{2k_o\cos\theta}$$

It should be noted that for <u>either</u> $|k_{ox}| > k_d$ <u>or</u> $|k_{oy}| > k_d$, the second term in (40) goes to zero very near grazing incidence because either $\xi_x = 0$ or $\xi_y = 0$ is not contained in (a_x,b_x) or (a_y,b_y). Equation (40) is now in a form suitable for comparison with the tilted plane Bragg formula which results from the conventional composite surface scattering theory. When the slopes of the large scale structure are large, i.e., $\overline{\zeta_{\ell x}^2}$ and $\overline{\zeta_{\ell y}^2} \gg 1$, it is not possible to

demonstrate a direct analytical comparison. However, when the slopes are small, it can be shown that the tilted plane Bragg scatter result is as follows, see [20];

$$\sigma^\circ(\theta,\pi) \approx \frac{2k_o^4}{\sqrt{\overline{\zeta_{\ell x}^2}\,\overline{\zeta_{\ell y}^2}}} \int_{-\infty}^{\infty}\int_{-\infty}^{\infty} g^2\, W(2k_o\cos\theta\tan\psi + 2k_o\sin\theta\,,\, 2k_o\cos\theta\tan\delta)$$

$$\cdot \exp\left[-\frac{\tan^2\psi}{2\overline{\zeta_{\ell x}^2}} - \frac{\tan^2\delta}{2\overline{\zeta_{\ell y}^2}}\right] d(\tan\psi)\, d(\tan\delta) \qquad (41)$$

where ϕ has been set equal to π, ψ and δ are tilt angles in and perpendicular to the plane of incidence, and the angle of incidence is restricted to greater than or equal to 30°. In obtaining (41), the small angle assumptions have been made, i.e. $\sin\psi \approx \tan\psi$, $\sin\delta \approx \tan\delta$. The g^2 coefficients depend upon the polarization of the incident field. For horizontal polarization,

$$g^2 \approx (\cos\theta - \sin\theta\tan\psi)^4 \left[1 + \frac{2\tan^2\delta}{\cos^2\theta\sin^2\theta} - \frac{\tan^2\delta}{\sin^2\theta}\right]^2 \qquad (42)$$

while for vertical polarization,

$$g^2 \approx \left[1 + (\sin\theta + \cos\theta\tan\psi)^2 + \mathrm{ctn}^2\theta\tan^2\delta\right]^2 \qquad (43)$$

and $g^2 = 0$ for cross polarization. With the correspondence $\xi_x \leftrightarrow \tan\psi$ and $\xi_y \leftrightarrow \tan\delta$, and setting $k_{ox} = 2k_o\sin\theta$ and $k_{oy} = 0$ in (40), there is a great deal of similarity between (40) and (41). One point of obvious disagreement is that (41) is <u>defined</u> as zero for $\theta \lesssim 30°$ while (40) has no such restriction. In the limit of zero large scale slope, (40) is zero for $2k_o\sin\theta < k_d$ because

the two integrations in (40) cancel each other. Thus, whereas (41) is rather arbitrarily limited to $\theta \gtrsim 30°$, the result in (40) has no angle limitation. Further comparisons of (40) and (41) could be accomplished for other situations, however, such an effort is pointless since (41) is clearly an approximation to (40).

When the large scale slopes are not small, the integrations in (40) must be accomplished numerically. In this case, the variation of R and Γ_{pp}^2, about the point $\xi_x = 0$, $\xi_y = 0$ are very important to the result. It is, therefore, possible that the cross polarized scattering may not be completely negligible especially near grazing incidence. For example, with $\phi = \pi$

$$\Gamma_{hv}^2(-\xi_x, -\xi_y) = \frac{4\xi_y^2 \xi_x^2 \cos^2\theta + 8\xi_y^2 \xi_x \sin\theta\cos\theta + 4\xi_y^2 \sin^2\theta}{1 + \xi_x^2 + \xi_y^2}$$

and

$$R(-\xi_x, -\xi_y) = \left\{ \frac{1}{2\sqrt{\pi}} \left[2\overline{\zeta_{\ell x}^2}\, \xi_x^2 + 2\overline{\zeta_{\ell y}^2}\, \xi_y^2 \right]^{1/2} \cdot \exp\left[-\frac{1}{2} \left\{ \frac{1}{\overline{\zeta_{\ell x}^2}\, \xi_x^2 + \overline{\zeta_{\ell y}^2}\, \xi_y^2} \right\} \right] \right.$$

$$\left. - \frac{1}{2} \operatorname{erfc}\left[\left\{ 2\overline{\zeta_{\ell x}^2}\, \xi_x^2 + 2\overline{\zeta_{\ell y}^2}\, \xi_y^2 \right\}^{-1/2} \right] + 1 \right\}^{-1} ,$$

the scattering will be directly dependent upon the large scale slopes. Thus, the first order perturbation solution gives rise to a depolarized component which is dependent upon the large scale slopes.

5.0 NUMERICAL EXAMPLE

Although the results obtained in section 3 present a formal solution to the problem of composite surface scattering, the question of how to choose k_d

requires further study. Since there is very little theoretical foundation for choosing k_d, other than $4k_o^2 \overline{\zeta_s^2} \ll 1$, this aspect of the problem is best dealt with by considering a specific example. To simplify matters somewhat, the surface height spectrum is taken to be isotropic; that is, $S(k_x,k_y)$ depends only on the distance between any two points in the $k_x k_y$ plane. For such a spectrum, $\overline{\zeta_{\ell x}^2} = \overline{\zeta_{\ell y}^2} = \overline{\zeta_{\ell t}^2}/2$ where $\overline{\zeta_{\ell t}^2}$ is the total mean square slope of the large scale structure, i.e. $\overline{\zeta_{\ell t}^2} = \overline{\zeta_{\ell x}^2} + \overline{\zeta_{\ell y}^2}$. The analysis will be further restricted to the case of $\overline{\zeta_{\ell t}^2}$ small. This condition permits the following approximation in (32), see the Appendix for a justification of this step;

$$R\left(\frac{k_{ox} - k_x}{2k_o \cos\theta}\ ,\ \frac{k_{oy} - k_y}{2k_o \cos\theta}\right) \approx R(0,0) = 1$$

$$\Gamma_{pp'}^2\left(\frac{k_{ox} - k_x}{2k_o \cos\theta}\ ,\ \frac{k_{oy} - k_y}{2k_o \cos\theta}\right) \approx \Gamma_{pp'}^2(0,0) \quad .$$

Converting from cartesian wavenumber space (k_x,k_y) to cylindrical coordinates (k,α) where $k_x = k\cos\alpha$ and $k_y = k\sin\alpha$, and substituting in (32) and (33) yields

$$\sigma_{pp'}^{\circ}(\theta,\phi) \approx \frac{\delta_{pp'}\sec^4\theta}{\overline{\zeta_{\ell t}^2}} \exp\left(-\frac{\tan^2\theta}{\overline{\zeta_{\ell t}^2}}\right)$$

$$+ \frac{4k_o^2 \sec^2\theta}{\overline{\zeta_{\ell t}^2}} \Gamma_{pp'}^2(0,0) \int_{k_d}^{\infty} S(k)\, I_o\left(\frac{k\sin\theta}{k_o \cos^2\theta\, \overline{\zeta_{\ell t}^2}}\right)$$

$$\cdot \exp\left[-\frac{(k - 2k_o\sin\theta)^2}{4k_o^2 \cos^2\theta\, \overline{\zeta_{\ell t}^2}} - \frac{k\sin\theta}{k_o\cos^2\theta\, \overline{\zeta_{\ell t}^2}}\right] k\,dk \qquad (44)$$

where the α-integration has been accomplished. The function $I_o(\cdot)$ is the Bessel function of the second kind. It should be noted that the integrations in (32) exclude a rectangular area in the $k_x k_y$-plane while the integral in (44) excludes a circular area. The difference can be avoided by redefining k_d in terms of the radial wavenumber coordinate and expressing the transform relation between $\overline{\zeta_s^2}\ \rho_r(\Delta k)$ and $S(k)$ as a Hankel transform. As in the case of (32), there is no restriction on θ for either term in (44) other than $\theta \leq \pi/2$.

For the surface height spectrum, the following specific form was selected;

$$S(k) = \begin{cases} \dfrac{Bk^4}{(k^2+\kappa^2)^4} & k \leq k_c \\ 0 & k > k_c \end{cases} \tag{45}$$

Equation (45) represents a polynomial approximation to the so-called Pierson-Moskowitz spectrum for the steady state response of the ocean surface to a surface wind of speed V. The constant κ is given by $(335.2\ V^4)^{-1/2}$, for k in $(cm)^{-1}$ and V in m/sec; this particular mixture of units is convenient for microwave scattering problems. The constant B was taken to be 0.0046. It should be emphasized that (45) was selected for example purposes and because expressions for the autocorrelation function exist [21]. No inference in regard to the characteristics of ocean backscattering is intended or implied since (45) is probably an overly simplistic description of the true surface. The spectrum of the large scale structure of the surface is equal to (45) for $k \leq k_d$ while the small scale undulations are represented by (45) for $k_d < k \leq k_c$. Since the wind speed dependent parameter κ is small for $V \gtrsim 2$ m/sec, the mean square height of the small scale surface perturbations is given by

$$\overline{\zeta_s^2} \approx \frac{B}{2}\left[\frac{1}{k_d^2} - \frac{1}{k_c^2}\right] \tag{46}$$

The constant β is defined as $4k_o^2\,\overline{\zeta_s^2} = \beta << 1$. Thus, using (46), the following relation for k_d is determined;

$$k_d^2 = \frac{2Bk_o^2 k_c^2}{\beta k_c^2 + 2B k_o^2} \tag{47}$$

Equation (47), therefore, defines k_d in terms of the electromagnetic wavenumber, k_o, the spectral constant, B, the spectral cutoff wavenumber, k_c, and the smallness parameter β. It can also be shown that the total large scale mean square slope has the form

$$\overline{\zeta_{\ell t}^2} \approx \frac{B}{2}\left[-\frac{11}{6} + \ell n\left(\frac{k_d^2+\kappa^2}{\kappa^2}\right)\right] \tag{48}$$

Unless otherwise stated, all subsequent results were accomplished with the arbitrary choice of $k_c = 12\ (cm)^{-1}$, and $k_o = 3.1416\ (cm)^{-1}$ $(\lambda_o = 2\ cm)$.

Thus, using (48) and (47), the cross section is entirely dependent upon the parameter β which, in turn, determines the size of the small scale mean square height $\overline{\zeta_s^2}$. If β is chosen to be 0.1, the resulting value of k_d (from (47)) is $0.95\ (cm)^{-1}$. Hence, for all surface features having a wavelength greater than or equal to 6.6 cm, the geometrical optics part of (44) is assumed to be an adequate description of the scattering process. Conversely, all surface features having a wavelength less than 6.6 cm are assumed to be responsible for the small scale diffraction described by the second term in (44). A typical result for V = 4.3 m/sec is shown in Figure 3 for horizontal polarization and in Figure 4 for vertical polarization. The solid curve in

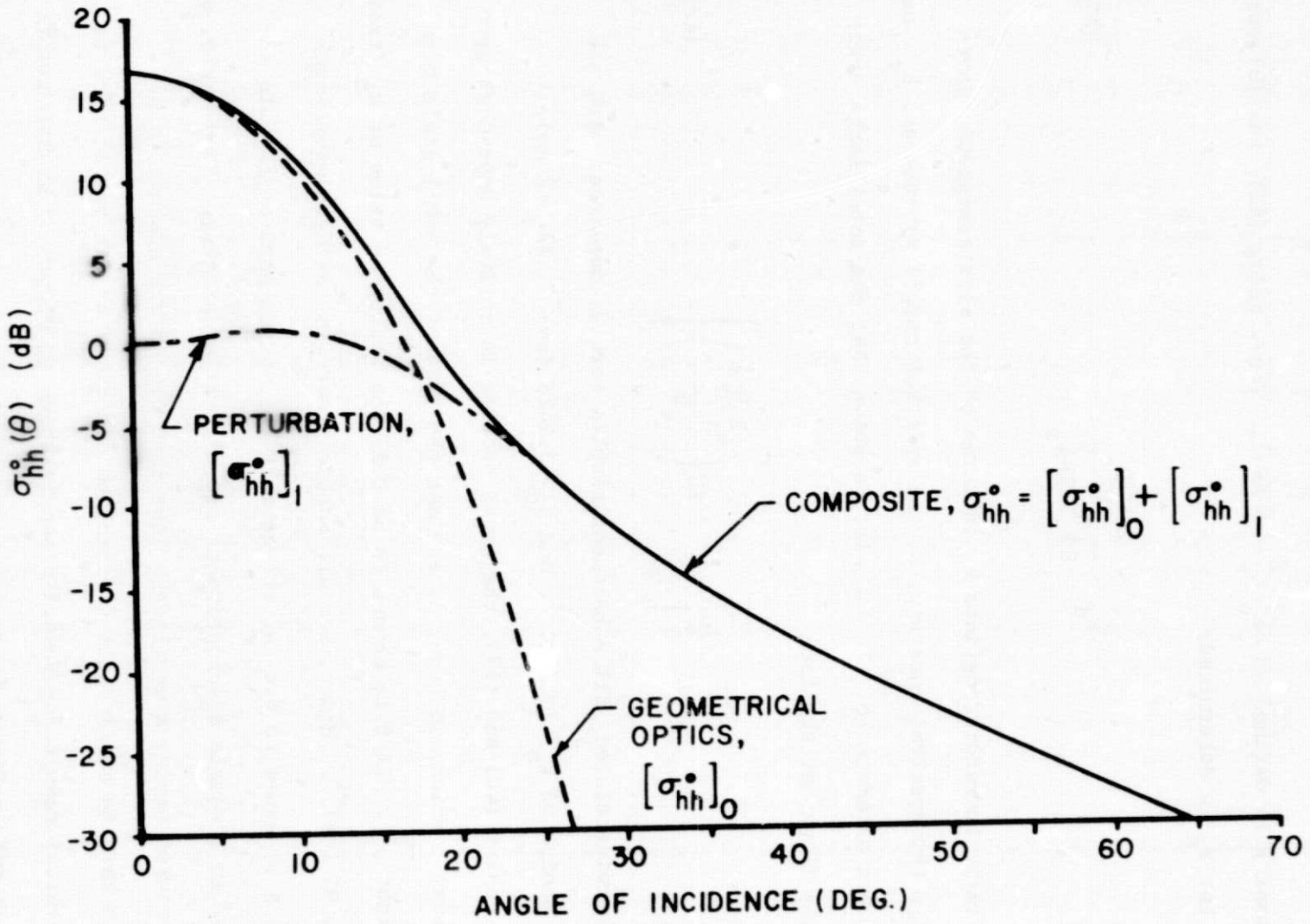

Figure 3. Backscattering cross section as a function of angle of incidence for horizontal polarization, $\lambda_o = 2$ cm, $V = 4.3$ m/sec, $k_d = 0.95$ (cm)$^{-1}$ ($\beta = 0.1$), and $\overline{\zeta_{\ell_t}^2} = 0.0224$.

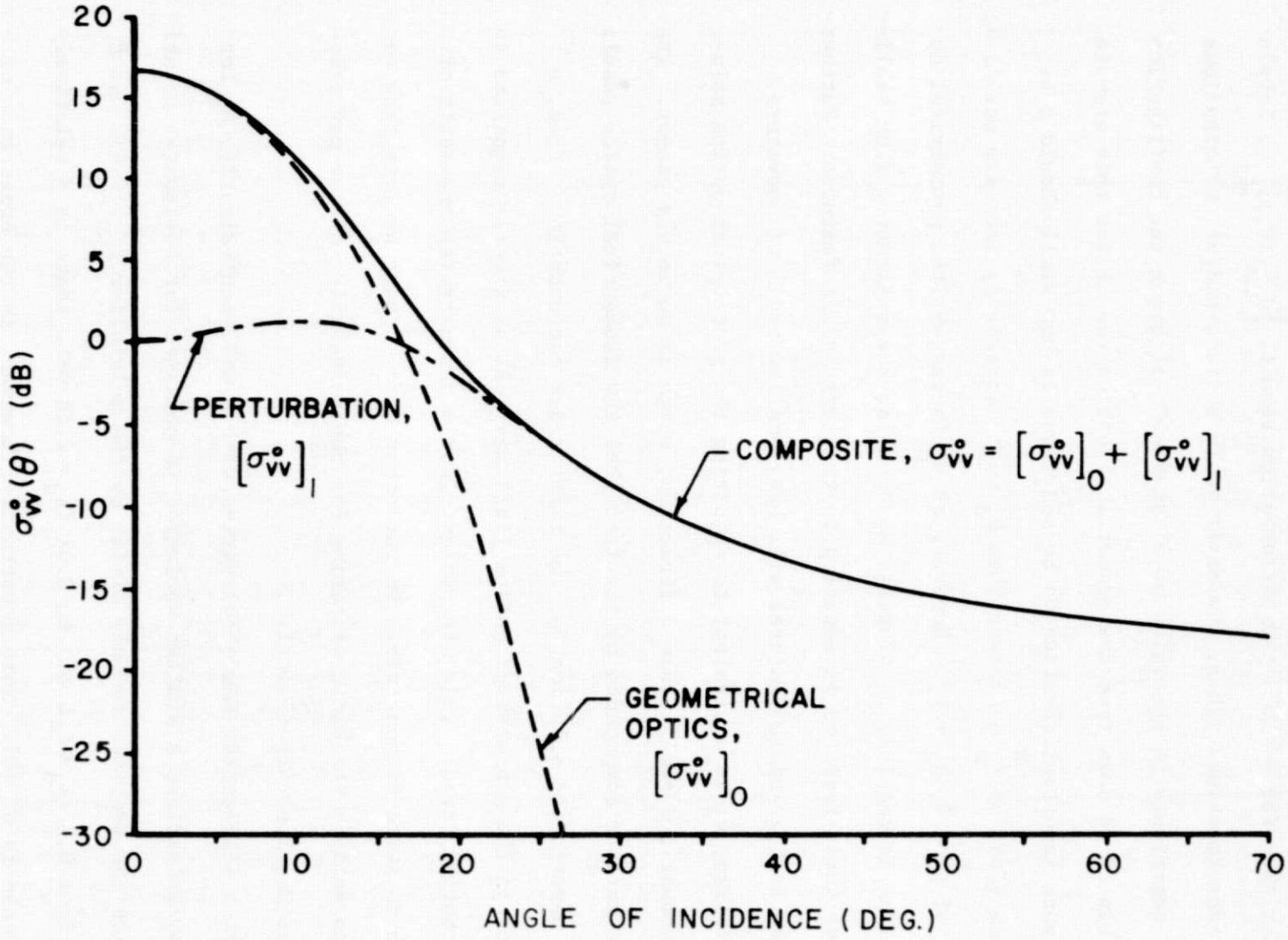

Figure 4. Backscattering cross section as a function of angle of incidence for vertical polarization, $\lambda_o = 2$ cm, $V = 4.3$ m/sec, $k_d = 0.95$ (cm)$^{-1}$ ($\beta = 0.1$), and $\overline{\zeta_{\ell_t}^2} = 0.0224$.

both figures is the sum of the two terms in (44) while the dashed curves show the individual contribution of each term. Of particular note in both figures is the fact that for $\theta \lesssim 10°$, the perturbation result, $\left[\sigma^{\circ}_{pp'}(\theta,\phi)\right]_1$, levels out to a nonzero value. Thus, the small scale surface height perturbations do indeed contribute to the value of σ° at $\theta = 0°$, although the contribution is more than 15 dB down from the geometrical optics result for this example.

The more important question to be addressed is how small should β be made. From (46), as $\overline{\zeta_s^2}$ decreases then k_d must necessarily increase until, in the limit of $\overline{\zeta_s^2} = 0$, $k_d = k_c$. However, as k_d increases, the geometrical optics solution is required to properly account for the scattering from smaller and smaller scale features in addition to the large scale features. Furthermore, these smaller scale features will have smaller radii of curvature. Thus, increasing k_d is equivalent to requiring the geometrical optics solution to account for small scale diffraction, which it obviously cannot. The problem is further compounded by the fact that the geometrical optics result forms the unperturbed solution for the first order perturbation. Thus, a small error in the geometrical optics field may well be greatly magnified in the perturbation field. This discussion clearly demonstrates the merit of choosing β as large as possible. On the other hand, β must be less than one in order to satisfy the basic criterion for the suitability of the perturbation technique, i.e. $4k_o^2 \overline{\zeta_s^2} \ll 1$.

Figure 5 illustrates how $\sigma^{\circ}(\theta)$ varies with β and, equivalently, k_d for vertical polarization; a similar variation is obtained for horizontal polarization since the two results only differ by the multiplier $\Gamma^2_{pp'}(0,0)$. As β decreases from 0.1 ($\lambda_d = 6.6$ cm) to 0.01 ($\lambda_d = 2.14$ cm), there is a relatively minor decrease in $\sigma^{\circ}_{vv}(0)$. More importantly, however, is the appearance of a

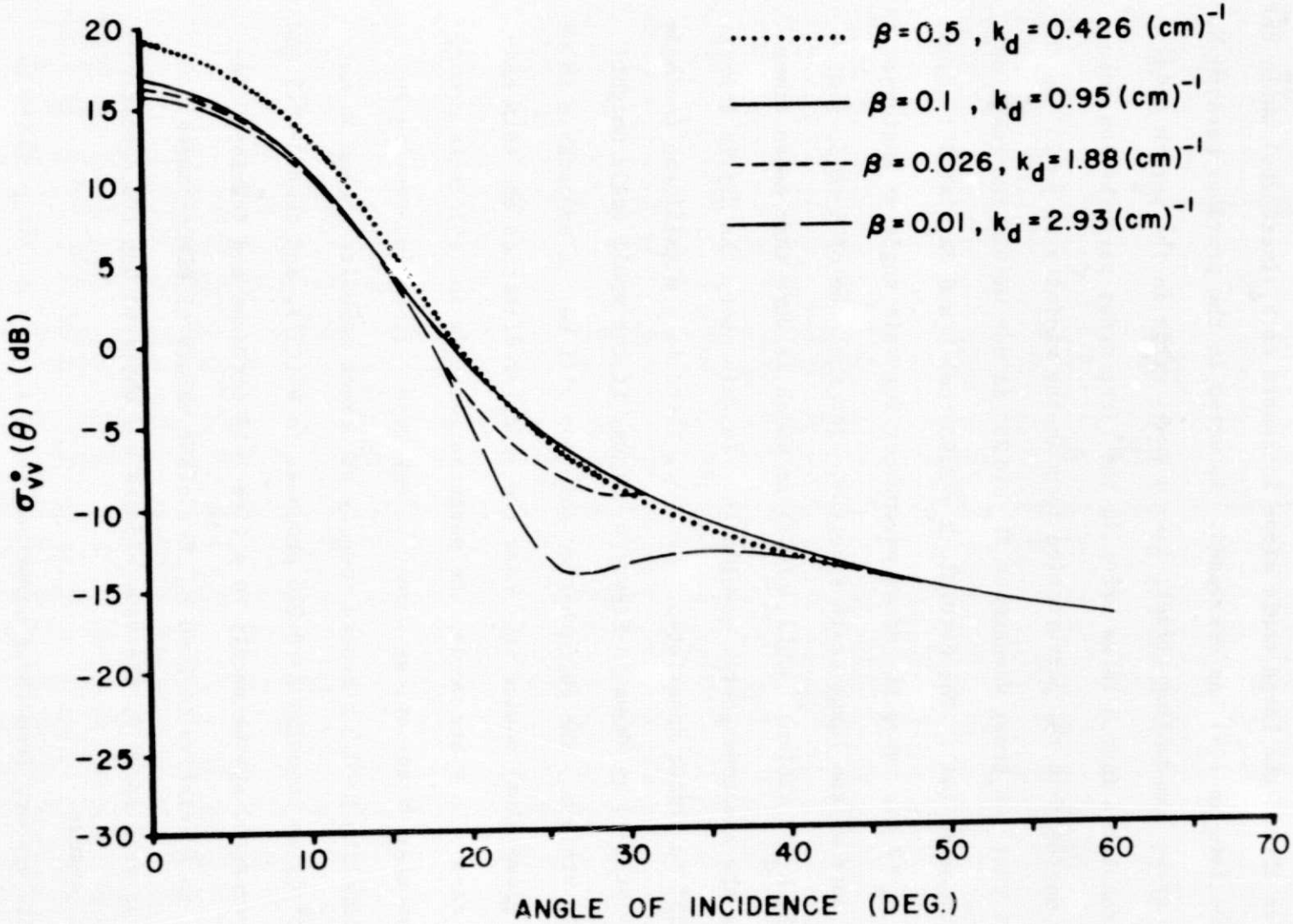

Figure 5. Variation in $\sigma^{\circ}(\theta)$ with truncation wavenumber k_d and β, for vertical polarization, $\lambda_o = 2$ cm, $V = 4.3$ m/sec, and $\overline{\zeta_s^2} = \beta/(4k_o^2)$.

dip in the vicinity of $\theta = 25°$. This dip results from the fact that the geometrical optics term in (44) is essentially negligible in the neighborhood of $\theta = 25°$ (even though the large scale slope increases as k_d increases) while the perturbation term in (44) has decreased. As noted in the previous paragraph, this is an error compounding effect, i.e. a small error in the zeroth order solution translates into a large error in the first order perturbation solution. The decrease in the perturbation term in the vicinity of $\theta = 25°$ is due to the fact that the Bragg wavenumber $2k_o \sin 25°$ is not within the range of the integration in (44). For $\beta = 0.01$, $k_d = 2.93\ (\text{cm})^{-1}$ and $2k_o \sin(25°) = 2.65\ (\text{cm})^{-1}$ for $\lambda_o = 2$ cm, thus, the Bragg wavenumber for this angle of incidence is actually a part of the large scale spectrum. For the case of $\beta = 0.5$, i.e. $4k_o^2 \overline{\zeta_s^2} = 0.5$, $k_d = 0.426(\text{cm})^{-1}$ and $\lambda_d = 14.75$ cm which is more than seven times as large as the electromagnetic wavelength. In this case, the dip in the vicinity of 25° is almost nonexistent; however, there is a significant increase in $\left[\sigma_{vv}^{\circ}(\theta)\right]_1$ at $\theta = 0$ as shown in Figure 6. Thus, if the small scale height criterion is violated, the perturbation solution will become comparable to or exceed the geometrical optics term near the specular direction and this cannot be the case. In other words, the perturbation term in (44) is in error, near the specular direction, as should be expected. It is interesting to note that choosing $\beta = 0.5$ produces roughly the exact opposite change in magnitude of $\sigma^{\circ}(0)$ as choosing $\beta = 0.026$ produces in $\sigma^{\circ}(25°)$, and that $\beta = 0.5$ and $\beta = 0.026$ correspond approximately to a five fold increase and decrease, respectively, in β relative to $\beta = 0.1$. For other values of electromagnetic wavelength or wind speed V, the same effects are observed but the specific numbers will change.

It would appear, from these numerical results, that a proper choice of

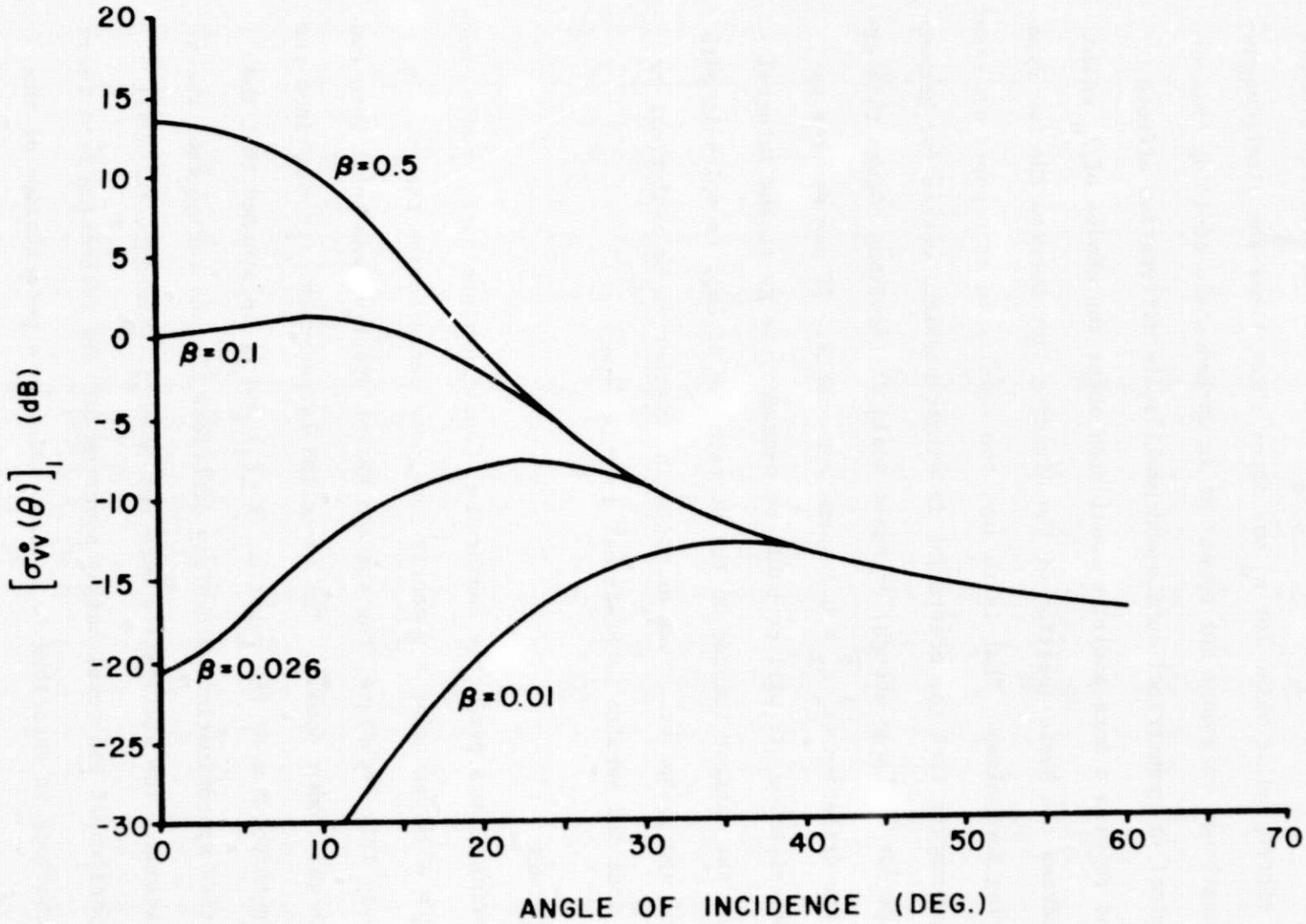

Figure 6. Variation of perturbation term with $\beta = 4k_o^2 \overline{\zeta_s^2}$ for vertical polarization, $\lambda_o = 2$ cm, V = 4.3 m/sec.

k_d should be based on the criterion $4k_o^2 \overline{\zeta_s^2} \approx 0.1$. For the spectrum studied here, the corresponding value for λ_d was about three times the electromagnetic wavelength and this does not appear as an unreasonable dividing line between physical or geometrical optics and small scale diffraction effects. Any attempt to draw a more positive conclusion about the choice of λ_d would have to address the basic question of the dividing line between the two types of scattering mechanisms. That is to say, the results in this paper are based upon the assumption that the scattering is either physical optics (or geometrical optics for k_o large enough) or small scale diffraction. Given this assumption, the criterion $4k_o^2 \overline{\zeta_\ell^2} \approx 0.1$ seems reasonable. If one desires to refine this criterion, it will probably be necessary to go to the integral equation for the current induced on the surface and attempt to solve it with a minimum of approximation. Such an approach, whether it be analytical or numerical, does not seem to be practical at this time.

6.0 CONCLUSIONS

Scattering from a perfectly conducting, Gaussian distributed, random surface has been analyzed using a recently developed perturbation theory. In order to apply this technique, the surface height spectrum was split into two parts in the wavenumber domain. The so-called large scale part comprises the long wavelength portion of the spectrum ($k \leq k_d$) and it is assumed that the physical optics approximation adequately describes the scattering from these height excursions. The small scale spectrum ($k > k_d$) represents the small wavelength portion of the total height spectrum and the scattering from these small perturbations is described to a first order by a perturbation of the large scale physical optics solution. The point of spectral dichotomy must

satisfy the relation $4k_o^2 \overline{\zeta_s^2} << 1$, where $\overline{\zeta_s^2}$ is the mean square height of the small scale structure.

A derivation of the expression for the scattering cross section, $\sigma^\circ_{pp'}(\theta,\phi)$, is presented for both anisotropic and isotropic surfaces for $4k_o^2 \overline{\zeta_\ell^2} >> 1$. To the accuracy of first order perturbation theory, the derivation is exact. The results are based on the evaluation of some complicated ensemble averages and spatial integrations appearing in previous publications. Shadowing of the large scale surface is included in the analysis. A direct comparison with the conventional composite surface scattering result when the large scale slopes are small, shows essentially identical agreement except in one regard - the result obtained here provides for a continuous transition from geometrical optics scattering to Bragg scattering rather than a piecewise continuous solution, i.e. the sum of two angle limited solutions. The result obtained here also indicates, directly in the spectral domain, the convolutional broadening of the Bragg line scattering by the presence of the large scale structure. When the large scale slopes are large, it is not possible to accomplish a direct analytical comparison between the conventional composite surface model and the results obtained here. However, such a comparison would only serve to check the conventional model since the present results are necessarily more accurate. For large slopes, it is shown that depolarization is possible but the results are directly dependent upon the slopes.

Numerical results are presented for a polynomial type surface height spectrum which is similar to the wind driven ocean spectrum. These results indicate a smooth transition between the geometrical optics and Bragg scattering regimes which previously have been obtained in an ad hoc fashion. Furthermore, these results show that the small scale structure does contribute a small

amount to the backscattering at normal incidence. For the spectral model chosen, the calculations and the physics of the problem both tend to indicate that the spectral division point k_d should be selected according to the criterion $4k_o^2 \overline{\zeta_s^2} \approx 0.1$. For $k_o = 3.14\ (\text{cm})^{-1}$, $k_d = 0.95\ (\text{cm})^{-1}$ and $\lambda_d = 6.6$ cm which is more than three times the electromagnetic wavelength. The value of λ_d also appears, physically, to be a reasonable dividing point between geometrical optics scattering and small scale diffraction.

REFERENCES

1. Barrick, D. E.; and Peake, W. H.: "A Review of Scattering From Surfaces With Different Roughness Scales," Radio Science, Vol. 3 (New Series), pp. 865-868, August, 1968.
2. Semenov, B.; "An Approximate Calculation of Scattering of Electromagnetic Waves From A Rough Surface," Radiotekhnika i Elektronika (USSR), Vol. 11, pp. 1351-1361, 1966.
3. Wright, J. W.: "A New Model For Sea Clutter," IEEE Trans. Antennas and Propagation, AP-16, pp. 217-223, March, 1968.
4. Fuks, I.; "Contribution to the Theory of Radio Wave Scattering on the Perturbed Sea Surface," Izvestia Vyshikh Uchebnikh Zavedenity, Radiofizika, Vol. 5, p. 876, 1966.
5. Fung, A. K; and Chan, H. L.: "Backscattering of Waves by Composite Rough Surfaces," IEEE Trans. Antennas and Propagation, Vol. AP-17, pp. 590-597, September, 1969.
6. Peake, W. H.; and Barrick, D. E.: "Comments on Backscattering of Waves by Composite Rough Surfaces," IEEE Trans. Antennas and Propagation, Vol. AP-18, pp. 716-720, September, 1970.
7. Burrows, M. L.; "A Reformulated Boundary Perturbation Theory In Electromagnetism and Its Application to a Sphere," Can. J. Phys., Vol. 45, pp. 1729-1743, May, 1967.
8. Burrows, M. L.; "Surface Tolerance of a Radar Calibration Sphere," IEEE Trans. Antennas and Propagation, Vol. AP-16, pp. 718-724, November, 1968.
9. Burrows, M. L.; "On the Composite Model for Rough Surface Scattering," IEEE Trans. Antennas and Propagation, Vol. AP-21, pp. 241-243, March, 1973.
10. Stogryn, A.; "Electromagnetic Scattering From Rough, Finitely Conducting

Surfaces," Radio Sciences, Vol. 2, pp. 415-428, April, 1967.

11. Evans, J. V.; and Hagfors, T.: Radar Astronomy, Chapter 5, McGraw-Hill Book Company, New York, 1968.

12. Hagfors, T.; "Relationship of Geometric Optics and Autocorrelation Approach to the Analysis of Lunar and Planetary Radar," J. Geophys. Res., Vol. 71, pp. 379-383, 1966.

13. Longuet-Higgins, M. S.; "The Statistical Analysis of a Random, Moving Surface," Phil. Trans. Roy. Soc. London, Vol. A249, pp. 321-387, February, 1957.

14. Beckmann, P.; "Scattering By Non-Gaussian Surfaces," IEEE Trans. on Antennas and Propagation, Vol. AP-21, pp. 169-175, March, 1975.

15. Sancer, M. I., "Shadow-Corrected Electromagnetic Scattering From A Randomly Rough Surface," IEEE Trans. on Antennas and Propagation, Vol. AP-17 pp. 577-585, September, 1969.

16. Barrick, D. E.; "Relationship Between Slope Probability Density Function and the Physical Optics Integral In Rough Surface Scattering," Proc. IEEE, Vol. 56, pp. 1728-1729, October, 1968 (also correction, Vol. 57, p. 256, February, 1969).

17. Brown, G. S. (Editor); "Skylab S-193 Radar Altimeter Experiment Analyses and Results," NASA CR-2763, Applied Science Associates, Inc., Apex, N. C., May, 1976.

18. Tyler, G. L.; "Wavelength Dependence In Radio-Wave Scattering and Specular Point Theory," Radio Science, Vol. 11, pp. 83-91, February, 1976.

19. Evgrafov, M. A.; Asymptotic Estimates and Entire Functions, Gordon and Breach Publ., New York, pp. 20-23, 1961.

20. Valenzuela, G. R.; Liang, M. B.; and Daley, J. C.: "Ocean Spectra For The High Frequency Waves As Determined From Airborne Radar Measurements," J. Marine Res., Vol. 29, pp. 69-84, February, 1971.

21. Miller, L. S.; Brown, G. S.; and Hayne, G. S.: "Analysis of Satellite Altimeter Signal Characteristics and Investigation of Sea-Truth Data Requirements," NASA CR-137465, Research Triangle Institute, Durham, N. C., April, 1972.

APPENDIX

The purpose of this Appendix is to justify the approximation that for small $\overline{\zeta_{\ell x}^2}$ and $\overline{\zeta_{\ell y}^2}$,

$$\left[\sigma^{\circ}_{pp'}(\theta,\phi)\right]_1 \approx \frac{k_o^2 \sec^2\theta}{\pi\left[\overline{\zeta_{\ell x}^2}\ \overline{\zeta_{\ell y}^2}\right]^{1/2}} R(0,0)\ \Gamma^2_{pp'}(0,0) \int_{-\infty}^{\infty}\int_{-\infty}^{\infty} S(k_x,k_y)$$

$$\cdot \exp\left[\frac{-(k_{ox}-k_x)^2}{8k_o^2\cos^2\theta\ \overline{\zeta_{\ell x}^2}} - \frac{(k_{oy}-k_y)^2}{8k_o^2\cos^2\theta\ \overline{\zeta_{\ell y}^2}}\right] dk_x\, dk_y$$

$$- \frac{k_o^2 \sec^2\theta}{\pi\left[\overline{\zeta_{\ell x}^2}\ \overline{\zeta_{\ell y}^2}\right]^{1/2}} R(0,0)\ \Gamma^2_{pp'}(0,0) \int_{-k_d}^{k_d}\int_{-k_d}^{k_d} S(k_x,k_y)$$

$$\cdot \exp\left[\frac{-(k_{ox}-k_x)^2}{8k_o^2\cos^2\theta\ \overline{\zeta_{\ell x}^2}} - \frac{(k_{oy}-k_y)^2}{8k_o^2\cos^2\theta\ \overline{\zeta_{\ell y}^2}}\right] dk_x\, dk_y \qquad (A1)$$

Under the following substitution;

$$\eta_x = \frac{k_x}{2k_o\cos\theta} \qquad \eta_y = \frac{k_y}{2k_o\cos\theta}$$

each of the terms in (32) are of the form

$$\frac{4k_o^4}{\pi\left[\overline{\zeta_{\ell x}^2}\ \overline{\zeta_{\ell y}^2}\right]^{1/2}} \int\int S\left(2k_o\cos\theta\,\eta_x,\ 2k_o\cos\theta\,\eta_y\right) R\left(\frac{k_{ox}}{2k_o\cos\theta}-\eta_x,\ \frac{k_{oy}}{2k_o\cos\theta}-\eta_y\right)$$

$$\cdot\ \Gamma_{pp}^2\left(\frac{k_{ox}}{2k_o\cos\theta}-\eta_x,\ \frac{k_{oy}}{2k_o\cos\theta}-\eta_y\right) \exp\left[-\frac{\left(\frac{k_{ox}}{2k_o\cos\theta}-\eta_x\right)^2}{2\overline{\zeta_{\ell x}^2}}-\frac{\left(\frac{k_{oy}}{2k_o\cos\theta}-\eta_y\right)^2}{2\overline{\zeta_{\ell y}^2}}\right] d\eta_x d\eta_y \qquad \text{(A2)}$$

When $\overline{\zeta_{\ell x}^2}$ and $\overline{\zeta_{\ell y}^2}$ are small, the Gaussian factor in (A2) is dominant and the integrals may be effectively truncated to a ± 4-sigma excursion about the peak in the Gaussian. That is, the limits in (A2) are essentially as given below;

$$\frac{k_{ox}}{2k_o\cos\theta}-4\sqrt{\overline{\zeta_{\ell x}^2}} \lesssim \eta_x \lesssim \frac{k_{ox}}{2k_o\cos\theta}+4\sqrt{\overline{\zeta_{\ell x}^2}}$$

$$\frac{k_{oy}}{2k_o\cos\theta}-4\sqrt{\overline{\zeta_{\ell y}^2}} \lesssim \eta_y \lesssim \frac{k_{oy}}{2k_o\cos\theta}+4\sqrt{\overline{\zeta_{\ell y}^2}} \qquad \text{(A3)}$$

For this set of limits, $R\Gamma_{pp}^2$, will vary from

$$R\left(4\sqrt{\overline{\zeta_{\ell x}^2}},\ 4\sqrt{\overline{\zeta_{\ell y}^2}}\right)\Gamma_{pp}^2\left(4\sqrt{\overline{\zeta_{\ell x}^2}},\ 4\sqrt{\overline{\zeta_{\ell y}^2}}\right) \qquad \text{(A4)}$$

to

$$R\left(-4\sqrt{\overline{\zeta_{\ell x}^2}},\ -4\sqrt{\overline{\zeta_{\ell y}^2}}\right)\Gamma_{pp}^2\left(-4\sqrt{\overline{\zeta_{\ell x}^2}},\ -4\sqrt{\overline{\zeta_{\ell y}^2}}\right) \qquad \text{(A5)}$$

as η_x and η_y vary over the range of integration. However, since the large

scale slopes are small, (A4) and (A5) do not appreciably depart from $R(0,0)\Gamma^2_{pp'}(0,0)$, and this product can be removed from inside the integrals as in (A1). The spectrum function, on the other hand, varies from

$$S\left(k_{ox} - 8k_o \cos\theta \sqrt{\overline{\zeta^2_{\ell x}}}\ ,\ k_{oy} - 8k_o \cos\theta \sqrt{\overline{\zeta^2_{\ell y}}}\right)$$

to

$$S\left(k_{ox} + 8k_o \cos\theta \sqrt{\overline{\zeta^2_{\ell x}}}\ ,\ k_{oy} + 8k_o \cos\theta \sqrt{\overline{\zeta^2_{\ell y}}}\right) \quad .$$

Since k_o is large, this variation may be significant, especially near $\theta = 0$. Thus, the spectrum function cannot, in general, be removed from under the integral in (A2). However, for θ sufficiently near to $\pi/2$ or grazing incidence, the spectrum can be removed since it will not significantly vary over the ranges of integration.

The above argument demonstrates that for small large scale slopes, the contribution to (A1) comes from a finite range of surface wavenumbers for θ near zero. Conversely, the contribution comes from a single wavenumber, i.e. (k_{ox}, k_{oy}), for θ near $\pi/2$ or grazing incidence.